Electronic Supplementary Material (ESI) for Sustainable Energy & Fuels.

Supplemental Information:

Enhanced Syngas Selectivity and Carbon Utilization during Chemical Looping Reforming of Methane via a Non-Steady Redox Cycling Strategy

Caroline M. Hill,[a] *Simon Ackermann,*[b] *Kathryn G. Trimm,*[a] *Dylan C. McCord,*[a] *Philipp Furler,*[b]
Jonathan R. Scheffe *[a]

[a] Department of Mechanical and Aerospace Engineering, University of Florida, Gainesville, USA, 32611
[b] Synhelion SA, Lugano, Switzerland, 6900
[*] Corresponding author. Phone: +1 352-392-0839; Email Address: jscheffe@ufl.edu

Table S1: Input parameters and operating conditions used for all thermodynamic modeling simulations.

Input Parameter	Value
Redox material	$CeO_{2-\delta}$
Temperature, T (°C)	800
Pressure, P (Pa)	101,325
Molar mass, M_s (g/mol)	172.115
Density, ρ_s (g/cm^3)	7.22
Sample mass, m_s (g)	1.0
Cross-section area, A (cm^2)	0.12
Bed length, L (cm)	7.62
Inlet flow rate, $\dot{n}_{\text{in}}$ (sccm)	100
Discretizations, N_D (-)	20 (1D) or 1 (spatially independent)

Table S2: Boundary and initial conditions for the simulations presented in Figure 2. The mole fraction of each species j is represented by y_j.

Case	Boundary Conditions	Initial Condition
Spatially Independent	$y_{\text{CH}_4}(t_k)\big\vert_{i=0} = 0.10$ $y_{\text{Ar}}(t_k)\big\vert_{i=0} = 0.90$ $y_j(t_k)\big\vert_{i=0} = 0$ all other species	$\delta(t_k)\big\vert_{k=0} = 0.025$
1D model constant δ_{start}	$y_{\text{CH}_4}(x_i,t_k)\big\vert_{i=0} = 0.10$ $y_{\text{Ar}}(x_i,t_k)\big\vert_{i=0} = 0.90$ $y_j(x_i,t_k)\big\vert_{i=0} = 0$ all other species	$\delta(x_i,t_k)\big\vert_{k=0} = 0.025$
1D model sloped δ_{start}	$y_{\text{CH}_4}(x_i,t_k)\big\vert_{i=0} = 0.10$ $y_{\text{Ar}}(x_i,t_k)\big\vert_{i=0} = 0.90$ $y_j(x_i,t_k)\big\vert_{i=0} = 0$ all other species	$\delta(x_i,t_k)\big\vert_{k=0} = 0.05 \cdot L$

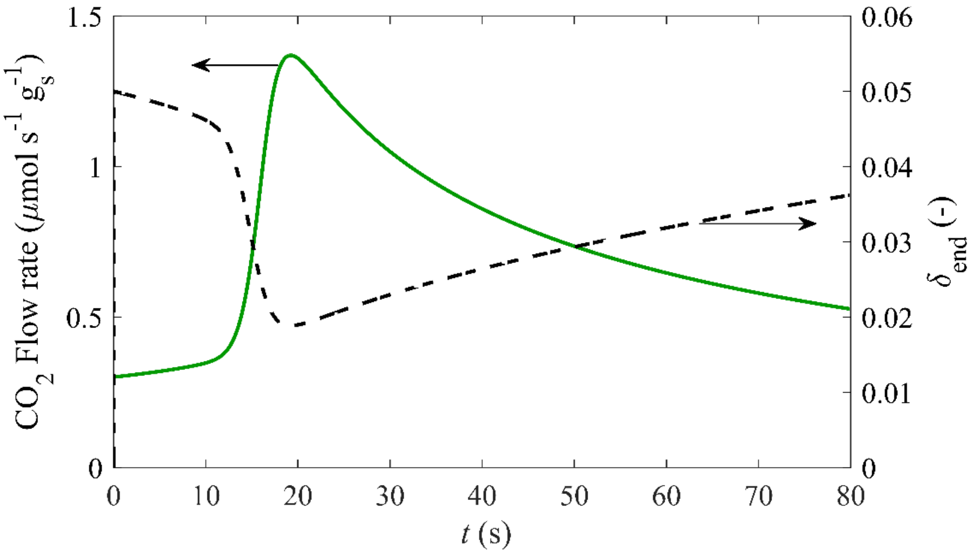

Figure S1: Specific CO_2 flow rate and δ_{end} as a function of t during the 1-D modeling simulation with sloped δ_{start} presented in Figure 2A. Input parameters and boundary conditions for this simulation are summarized in supplemental Tables S1 and S2.

Based on Figure S1, the correlation between molar flow rate of CO_2 ($\dot{n}_{\mathrm{CO2}}$) and δ_{end} shown in Equation S1 was extracted. Comparison to the other modeling cases presented in the main body indicates this correlation is a good fit for all simulations conducted with the same input parameters and operating conditions.

$$\delta_{\mathrm{end}}(\dot{n}_{\mathrm{CO_2}}) = 0.05446\cdot\exp(-4.135\cdot\dot{n}_{\mathrm{CO_2}}) + 0.04057\cdot\exp(-0.5699\cdot\dot{n}_{\mathrm{CO_2}}) \tag{S1}$$

The experiments presented in Figure 6 were conducted in a fixed bed reactor under the same operating conditions and reactor geometry as the above correlation, with the exception that Ni promoted $CeO_{2-\delta}$ was utilized in the experimental demonstration to improve kinetics. If the added Ni is assumed to have minimal effect on the thermodynamic properties of $CeO_{2-\delta}$, the correlation presented in Equation S1 may be used to estimate δ_{end} during the reduction half-reactions of each experimental demonstration. These results are shown in Figure S2. Note that these predictions are based on the thermodynamic model and are thus subject to inaccuracies due to the model assumptions (i.e., no kinetic limitations, limited considered species, constant temperature and pressure, etc.). However, results still provide insight into the qualitative behavior of δ_{end}.

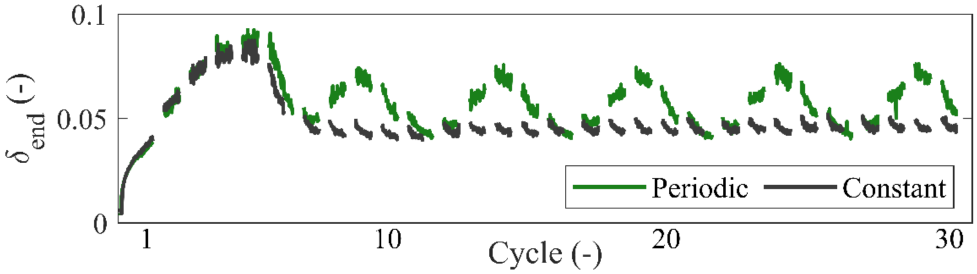

Figure S2: Estimated δ_{end} during each reduction step for the two experiments presented in Figure 6. The response of δ_{end} was extracted by applying the correlation shown in Equation S1 to the measured specific CO_2 flow rates.

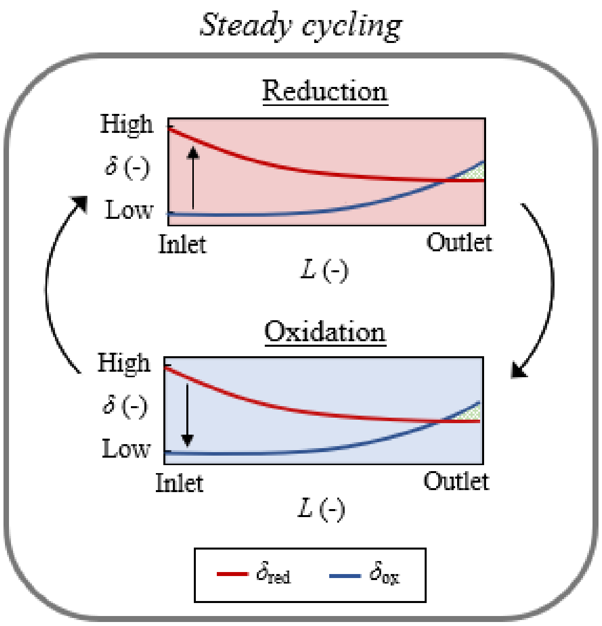

Figure S3: Schematic of the expected δ profiles during CLRM with constant reaction times after steady cycling is obtained. The δ profile as a function of reactor bed length after the reduction step (i.e., δ_{red}) and the oxidation step (i.e., δ_{ox}) are shown in red and blue, respectively. During the reduction step, shown on top and highlighted in red, the front portion of the bed is reduced upon exposure to methane and the subsequent product species. However, the end portion of the fixed bed is at higher δ before reduction and, under some conditions, is favorable to oxidize. Thus, δ_{end} may decrease during reduction despite δ_{avg} increasing overall. The reverse occurs during the oxidation reaction, shown on the bottom and highlighted in blue. The front portion of the fixed bed is oxidized upon exposure to high concentrations of CO_2 and/or H_2O at the inlet, resulting in an overall decrease in δ_{avg}. However, assuming most of the oxidant reacts in the front portion of the bed, the latter portion of the bed is exposed to high concentrations of CO and/or H_2. As a result, reduction of the redox material is more favorable and δ_{end} increases slightly during oxidation.

The correlation used to determine n_{H2} in Equation 8 is listed in Equation S2. This correlation was derived from thermodynamic chemical equilibrium calculations for the reaction of methane with CeO_2 in a single control volume and is solely a function of reaction temperature (T).

$$f(T) = -1.986894680506529 \times 10^{-9} \cdot T^{3} + 8.604917356529941 \times 10^{-6} \cdot T^{2} \\ -0.008318461099731075 \cdot T + 2.3964458139367935 \tag{S2}$$

Figure S4 presents a direct comparison between δ_{avg} and S_{H2} determined using the above correlation vs. direct measurement of n_{H2} during a CLRM experiment at 700 °C with steady high δ_{avg}. Notably, use of the correlation method has minimal effect on δ_{avg}. After the initial reduction, δ_{avg} deviates less than 0.01 and the difference decreases over time. While the magnitude of S_{H2} is significantly for the two methods, the overall trend is relatively constant for both.

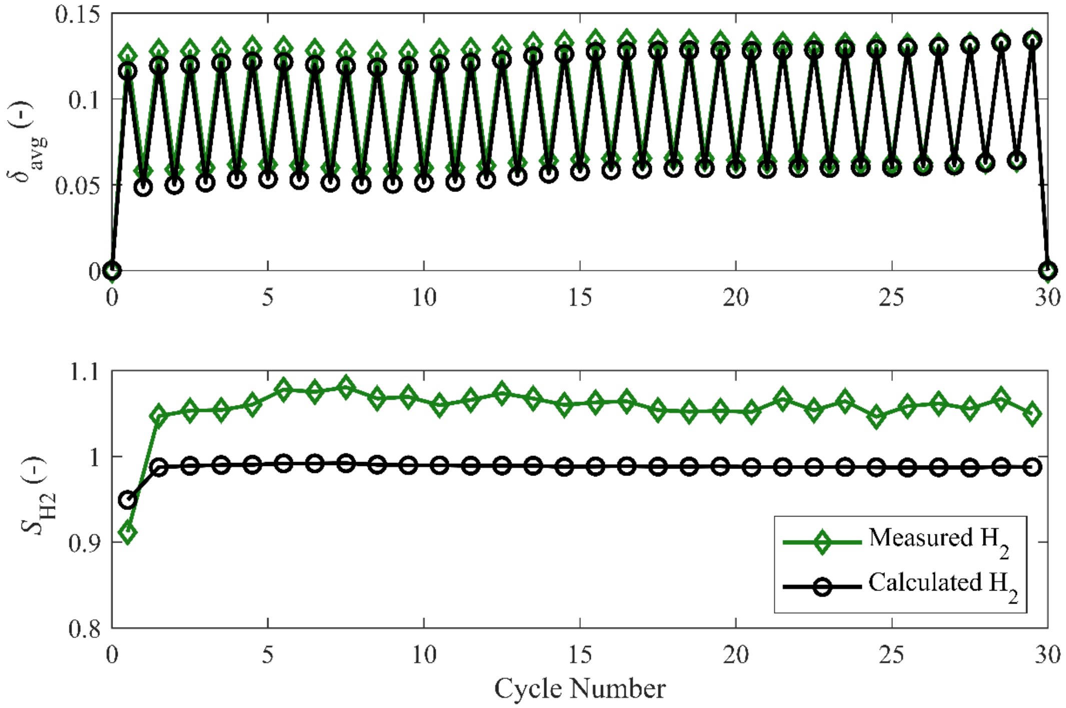

Figure S4: Comparison of A) δ_{avg} and B) S_{H2} during 30 CLRM cycles at 700 °C determined using measured (green) vs. correlated (black) values of n_{H2}. Reaction times for this experiment are as follows: $t_{red,1}$ = 90s, t_{red} = 60s, and t_{ox} = 109s.

A comparison of the correlation method to experimental results presented by Warren et al.[1] and Fosheim et al.[2] is shown in Figure S5. In most cases, n_{H2} values predicted by the thermodynamic correlation method (blue diamonds) do not fall within the uncertainty range of reported n_{H2}. However, if uncertainties for all other measured species ($n_{CH4,in}$, n_{CH4}, n_{CO}, and n_{CO2}) used by the correlation method are included in the calculations, uncertainty in the predicted n_{H2} values overlaps with the reported ranges. This comparison points out the high degree of uncertainty in calculating n_{H2} values using the correlation method but also confirms that the correlation method is valid and n_{H2} will follow the same trends as measured values.

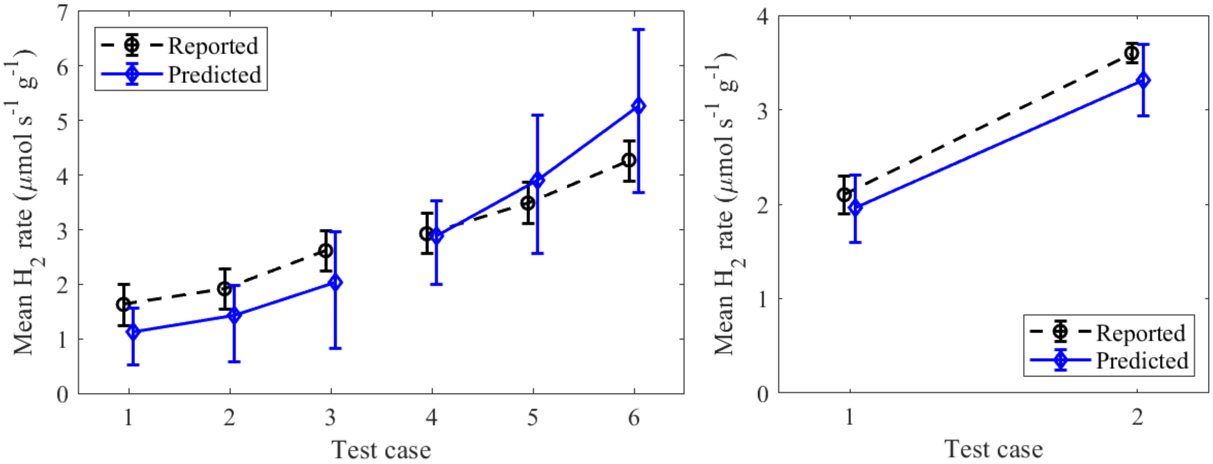

Figure S5: Comparison of n_{H2} values predicted by the correlation method to measured n_{H2} values reported in other published work. A) Cases 1-6 correspond to n_{H2} presented in Figure 5 of Warren et al.[1] B) Cases 1 and 2 correspond to Test 1 and 2 presented in Table 2 by Fosheim et al.[2]

References:

1 K. J. Warren, R. J. Carrillo, B. Greek, C. M. Hill and J. R. Scheffe, *Energy Technology*, 2020, **8**, 2000053.

2 J. R. Fosheim, B. J. Hathaway and J. H. Davidson, *Energy*, 2019, **169**, 597–612.